

How Many Elementary Processes Are Involved in Base- and Acid-Promoted Aldol Condensations?

Shinichi Yamabe,^{*,[a]} Kohji Hirahara,^[a] and Shoko Yamazaki^[a]

Keywords: Aldol reactions / Reaction mechanisms / Density functional calculations / Hydrogen bonds / Aldehydes

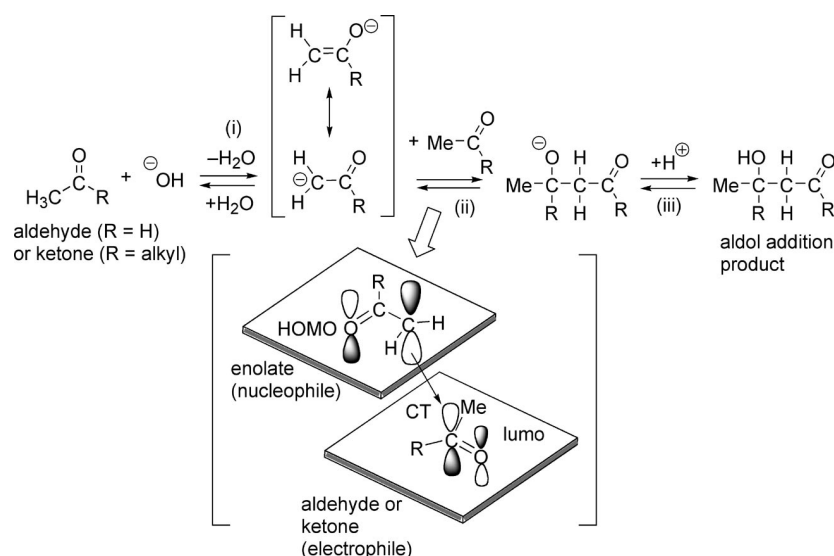
The title reactions were investigated by density functional theory calculations. $\text{MeRC=O} + \text{OH}^- + (\text{H}_2\text{O})_8$ ($\text{R} = \text{H}$ and Me) and $\text{MeCH=O} + \text{H}_3\text{O}^+ + (\text{H}_2\text{O})_8$ systems were adopted to trace the elementary processes. Eight water molecules were included to assure proton shifts through hydrogen bonds. The OH^- -containing reactions were confirmed to have three elementary processes. Whereas the rate-determining step of

the reaction of acetaldehyde is C–H bond scission, that of acetone is C–C bond formation. The H_3O^+ -containing reactions have two elementary processes. The reactivity difference between OH^- - and H_3O^+ -promoted reactions was discussed in terms of their mobility and hydration strength. (© Wiley-VCH Verlag GmbH & Co. KGaA, 69451 Weinheim, Germany, 2007)

Introduction

Aldol is a combined term of aldehyde–alcohol, and the aldol condensation reaction was discovered in 1872.^[1] The classic aldol reaction is base-catalyzed, where an enolate adds to an aldehyde or ketone (Scheme 1). It is also possible to use acid catalysis, where in the initial step the carbonyl substrate undergoes tautomerization to the enol and in the

subsequent step the enol adds to the protonated carbonyl compound (Scheme 2).^[2] The aldol reaction is in equilibrium, which may lie either to the right (product) or to the left (reactant) depending on the adopted substrates (aldehydes and/or ketones). In the case of CH_3CHO in Scheme 1, the equilibrium is found to lie favor of the aldol product. The forward reaction of step (ii) and the reversal of step (i) are essentially competing with each other for the

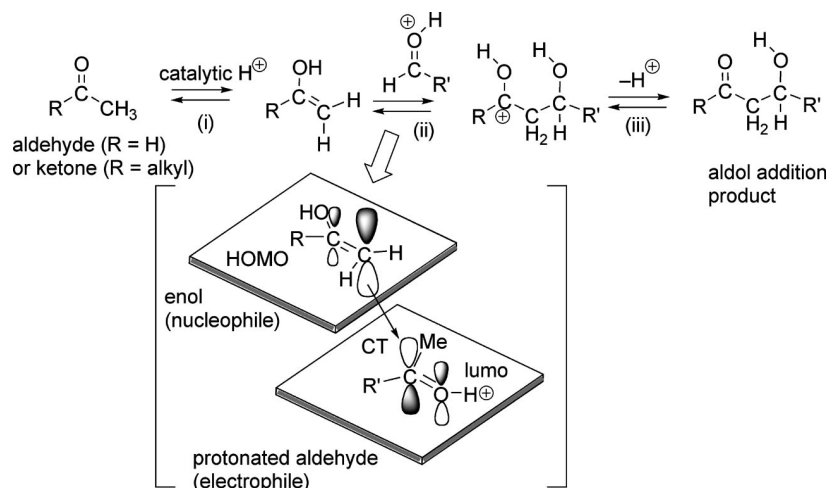


Scheme 1. The base-promoted aldol reaction. CT is the charge transfer from the HOMO of the enolate to the lumo of the aldehyde or ketone.

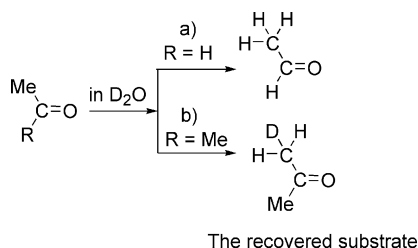
[a] Department of Chemistry, Nara University of Education, Takabatake-cho, Nara 630-8528, Japan
E-mail: yamabes@nara-edu.ac.jp

Supporting information for this article is available on the WWW under <http://www.eurjoc.org> or from the author.

enolate. Carrying out the reaction in D_2O fails to result in the incorporation of any deuterium into the CH_3 group of as-yet recovered acetaldehyde (Scheme 3a). Therefore, step (ii) must be so much more rapid than the reverse of step (i) as to make the latter virtually irreversible.^[3]



Scheme 2. The acid-promoted aldol reaction. CT is the charge transfer from the HOMO of the enol to the lumo of the protonated aldehyde.



Scheme 3. After the base-promoted aldol reaction, absence or presence of deuterium in the methyl group of the recovered substrate.

In contrast, even for simple ketones, for example, acetone ($R = \text{CH}_3$), the equilibrium is found to lie far to the left ($\approx 2\%$ of the product). Thus, if the reaction of acetone is carried out in D_2O , incorporation of deuterium into the CH_3 group of as-yet unchanged acetone is observed. That is, step (ii) is no longer rapid with respect to the reversal of step (i) (Scheme 3b).

Although the classic aldol reaction is a fundamental one (only C, H, and O atoms included), its detailed mechanism has not been elucidated. It is a question of how many elementary processes are involved in base- and acid-promoted reactions. In both reactions, proton release or attainment in the substrate should take place through hydrogen bonds. Then, the mechanism needs to be considered in terms of the correlation between covalent bond formation and proton relays along the hydrogen bonds. Computational studies are expected to reveal the correlation by simulating reaction paths. However, there have been no reports dealing with elemental ($\text{MeCHO} + \text{H}_2\text{C}=\text{CHO}^-$) or ($\text{MeCHO} + \text{MeCHOH}^+$) systems. Tomasi et al. pointed out the importance of water in the aldol reaction between acetaldehyde and vinyl alcohol.^[4] In the neutral reaction, a water molecule was found to lower the activation energy. Al-

though only one H_2O molecule was included to trace the reaction path, the calculated result suggests the need of hydrogen-bonded H_2O clusters to construct reaction models.

In this work, base- and acid-promoted aldol reactions of acetaldehyde were investigated by including $\text{OH}^-(\text{H}_2\text{O})_8$ and $\text{H}_3\text{O}^+(\text{H}_2\text{O})_8$ so as to reveal the mechanism. A $\text{Me}_2\text{C}=\text{O}\cdots\text{OH}^-(\text{H}_2\text{O})_8$ system was also examined. Particular interest is in the number of elementary processes of H_3O^+ - and OH^- -containing reactions. These ions are known to move more rapidly than other ions between the cathode and anode in aqueous solution (Table 1).^[5]

Table 1. Rates, u_+ , and u_- , of typical ions in the electrode (aqueous solution).^[5]

Cation	$u_+ \times 10^4$ [$\text{cm}^2 \text{s}^{-1} \text{V}^{-1}$]	Anion	$u_- \times 10^4$ [$\text{cm}^2 \text{s}^{-1} \text{V}^{-1}$]
H_3O^+	36.25	OH^-	20.55
Li^+	4.01	F^-	5.74
Na^+	5.19	Cl^-	7.91
K^+	7.62	Br^-	8.09

The values of $u_+(\text{H}_3\text{O}^+)$ and $u_-(\text{OH}^-)$ are much larger than rates of other ions, which indicates proton relays in the H_3O^+ and OH^- movement. There is a question of whether the difference between $u_+(\text{H}_3\text{O}^+) = 36.25 \times 10^{-4} \text{ cm}^2 \text{s}^{-1} \text{V}^{-1}$ and $u_-(\text{OH}^-) = 20.55 \times 10^{-4} \text{ cm}^2 \text{s}^{-1} \text{V}^{-1}$ is reflected in the reactivity difference of base- and acid-promoted reactions. The $\text{H}_3\text{O}^+\cdots\text{H}_2\text{O}$ bonding energy was obtained both experimentally^[6] and theoretically^[7] to be 36 kcal mol^{-1} . The $\text{OH}^-\cdots\text{H}_2\text{O}$ energy was computed by RB3LYP/6-311+G* to be 28 kcal mol^{-1} . It is also a question of how the energy difference is reflected in the reactivity.

Method of Calculations

The reacting systems were investigated by density functional theory calculations. The B3LYP method^[8] was used. B3LYP seems to be a suitable method, because it includes the electron correlation effect to some extent. The basis set employed was 6-31(+)G* (for the OH⁻-containing system, diffuse orbitals on oxygen atoms) and 6-31G* (for the H₃O⁺-containing system). Then, the geometry optimizations were carried out by RB3LYP/6-31(+)G* or 6-31G*.

Transition states (TSs) were characterized by vibrational analysis, which checked whether the obtained geometries have single imaginary frequencies (ν^\ddagger). From the TSs, reaction paths were traced by the intrinsic reaction coordinate method^[9] to obtain the energy-minimum geometries. Relative Gibbs free energies were refined by single-point calculations of RB3LYP/6-311+G(d) [self-consistent reaction field (SCRf) = dipole, solvent = water]^[10] on the RB3LYP/6-31(+)G* geometries and thermal correction ($T = 300$ K, $P = 1$ atm) energies. Although more sophisticated SCRf methods such as SCRf = PCM and SCRf = IEFPCM are desirable, sizes of the reaction systems treated in this study are large and TSs with incomplete covalent bonds could not be calculated by those methods. Therefore, the SCRf = dipole method was used for single-point calculations.

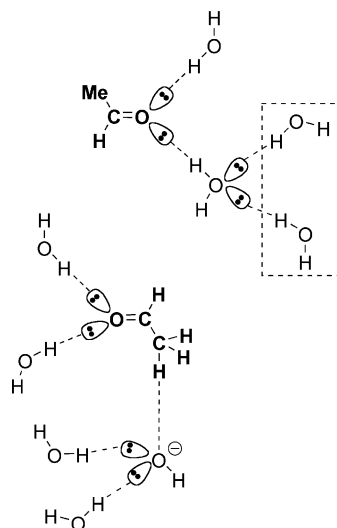
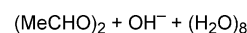
All the calculations were carried out by using the GAUSSIAN 03^[11] program package. The computations were performed at the Research Center for Computational Science, Okazaki, Japan.

Results and Discussions

The Base-Promoted Reaction

Scheme 4 presents a reaction model to trace the reaction path. Water molecules are bound to lone pair orbitals of the substrate (MeCHO) and the base (HO⁻). Figure 1 shows the path. In the "precursor" (before reaction), two MeCHO molecules are linked through hydrogen bonds and the hydroxide ion O15–H16 is surrounded by water molecules. When O15–H16 is in contact with a methyl hydrogen H5, the first transition state (TS1) is brought about. At TS1, the O15...H5 distance is 1.318 Å and that of H5...C3 is 1.337 Å. After TS1, the first intermediate, Int1, is formed. Int1 is composed of the enolate H₂C=CHO⁻, MeCHO, and (H₂O)₉. The enolate oxygen O2 is hydrogen-bonded strongly to H24 and H34. As the geometry of Int1 is not ready for subsequent C...C bond formation, a conformer of Int1 was sought. The conformer Int2, which is slightly more stable than Int1, was found. In Int2, the C3...C8 distance is 3.273 Å, which is usual for a weak interactive complex. After Int2, TS2 was obtained, where the C...C distance (2.004 Å) is within the typical value (1.9–2.5 Å) for the transition state.^[12] O9–C8...C3–C1 is antiperiplanar (the dihedral angle is -179.71°). Consequently, the one-center adduct, Int3, was obtained. In Int3, the C8–O9 moiety is an alkoxide, and it is tightly hydrogen bonded to H22 (O9...H22 1.396 Å). The movement of H22 toward O9 leads

to TS3, which affords the aldol product. Thus, the OH⁻-catalyzed aldol reaction of (MeCHO)₂ consists of three elementary processes, precursor \rightarrow TS1 \rightarrow Int1 \rightleftharpoons Int2 \rightarrow TS2 \rightarrow Int3 \rightarrow TS3 \rightarrow product.



Scheme 4. A reaction model of the base-promoted aldol condensation. Water molecules are bonded to lone pair orbitals. Two H₂O molecules in the broken-line box are included to provoke the hydrogen bond circuit during the condensation.

Figure 2 exhibits a reaction of (acetone)₂, OH⁻, and (H₂O)₈. The optimized geometries of precursor, TS1, Int1, Int2, TS2, Int3, TS3, and product were computed to be similar to those in Figure 1. The similarity demonstrates that the methyl substitution to MeCHO (i.e., MeCHO \rightarrow Me₂CO) does not affect the reaction path significantly.

Figure 3 shows changes of Gibbs free energies ($T = 298$ K, $P = 1$ atm). Whereas geometries in Figures 1 and 2 are similar, the energy changes are drastically different. Whereas the rate-determining step of the (MeCHO)₂ reaction is TS1, that of the (Me₂CO)₂ reaction is TS2. The energy of TS2(Me₂CO) is larger than that of TS1(MeCHO), and the energy of product (Me₂CO) is larger than that of product (MeCHO). Thus, acetone has a lower reactivity than acetaldehyde, which is consistent with the experimental evidence. The difference in the rate-determining step, TS1(MeCHO) versus TS2(Me₂CO), is in accord with the experimental contrast shown in Scheme 3. The deuterium incorporation to the methyl group of the unreacted substrate is possible for acetone in the equilibrium: precursor \rightleftharpoons Int2 (before the rate-determining step TS2). In contrast, it is impossible for acetaldehyde, because transit of the rate-determining step TS1 does not allow the reverse route, Int2 \rightarrow precursor.

The energy difference for the two first steps of the aldol reactions with acetaldehyde and acetone is discussed. Although TS2(at) is located 6.5 kcal mol⁻¹ over TS2(al), the activation free energy difference for the two elementary steps is only of 3.31 kcal mol⁻¹ as a consequence of the

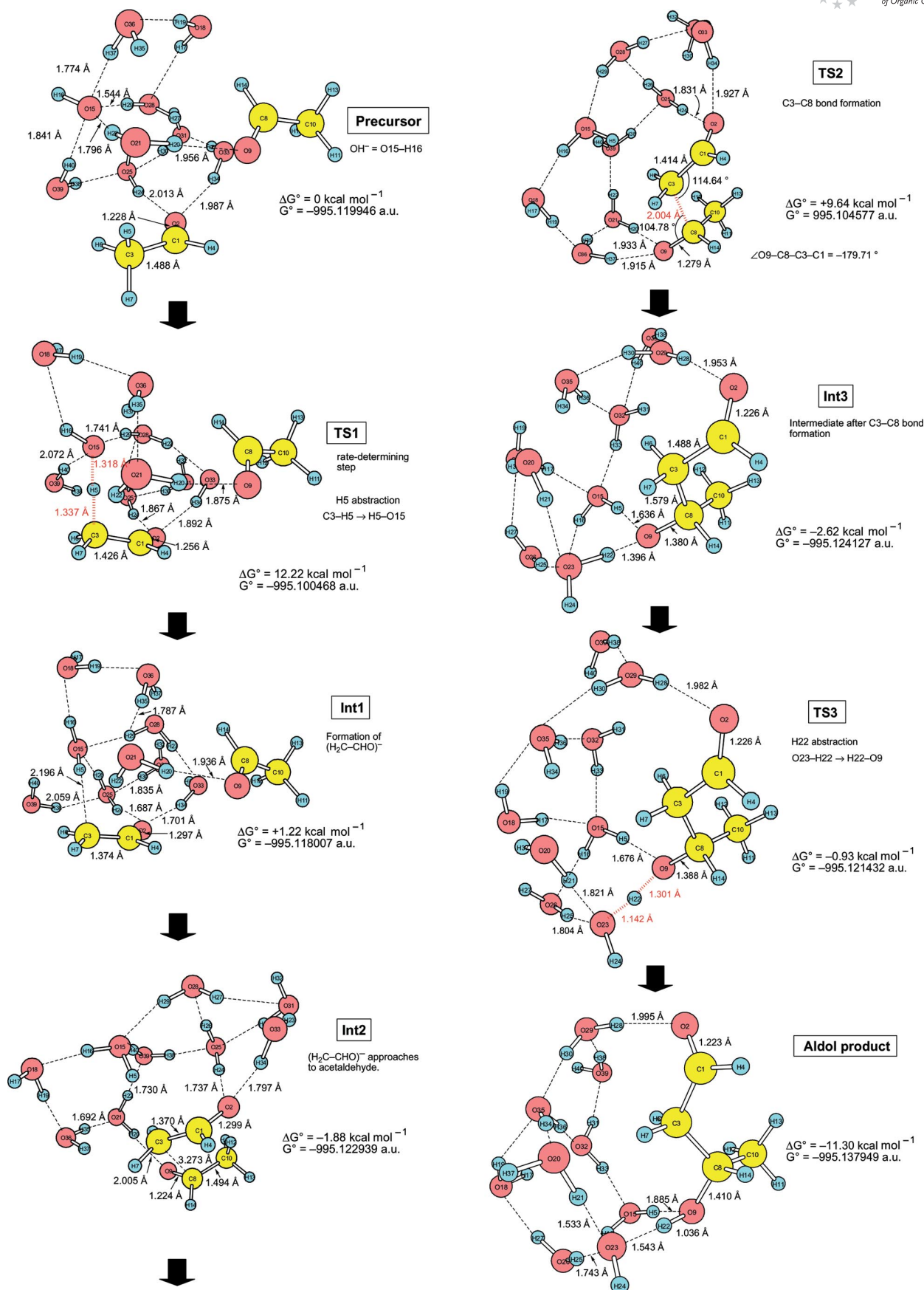
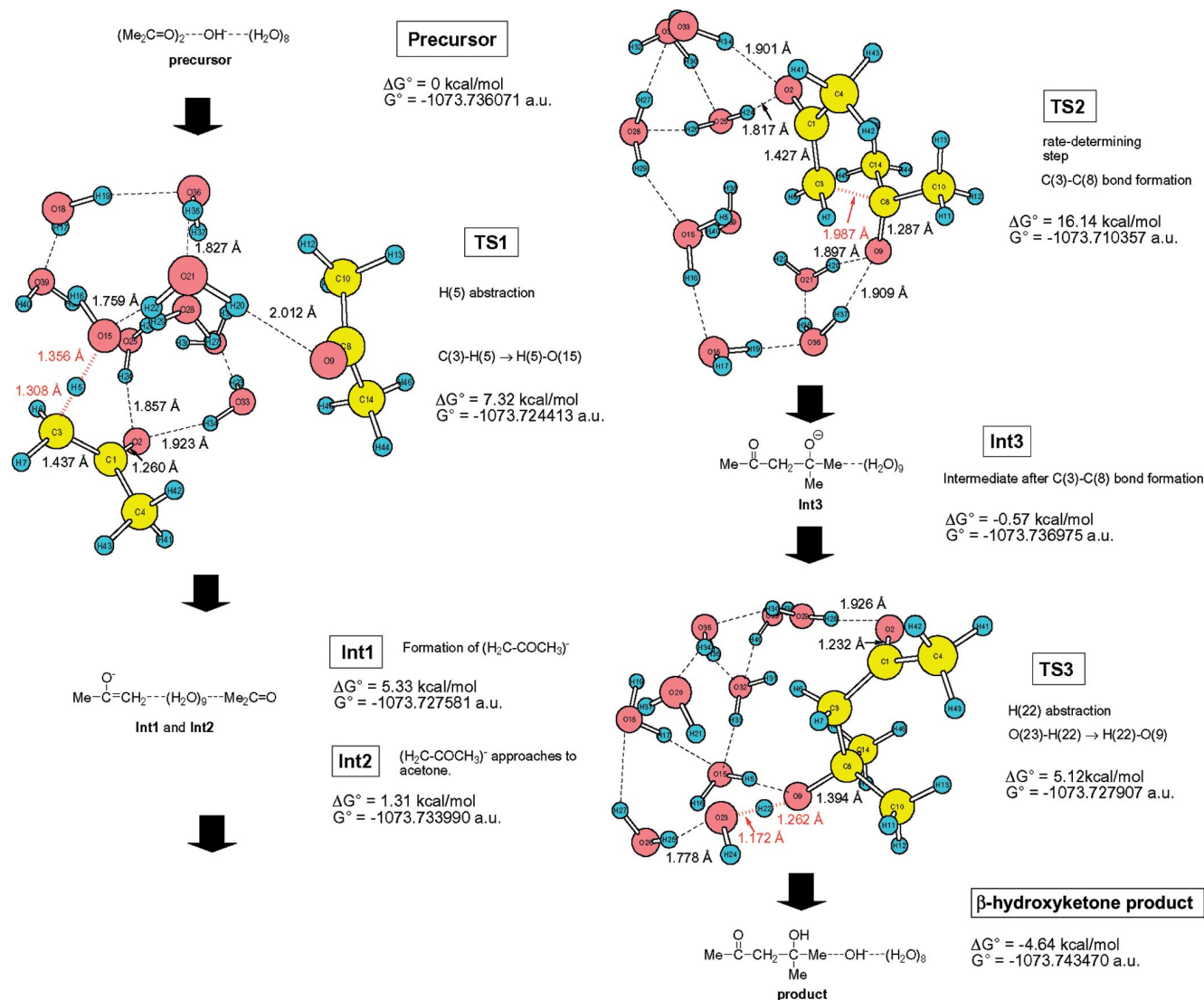
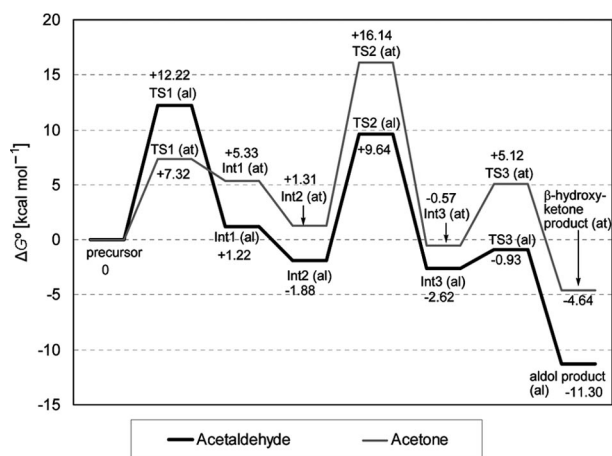
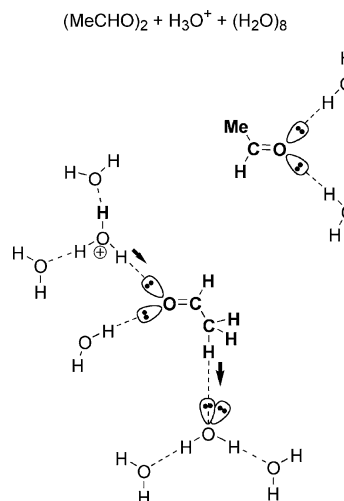


Figure 1. Geometric changes in the base-catalyzed aldol reaction of $(\text{MeCHO})_2 + \text{OH}^- + (\text{H}_2\text{O})_8$ in Scheme 4. Int1, Int2, and Int3 are intermediates.

Figure 2. Three TS geometries of the base-catalyzed aldol reaction of $(\text{acetone})_2 + \text{OH}^- + (\text{H}_2\text{O})_8$.Figure 3. Energy diagrams of Gibbs free energies ($T = 298.15 \text{ K}$ and $P = 1 \text{ atm}$) along the OH^- -promoted reactions of Figures 1 and 2; "al" and "at" in parentheses stand for the energies of acetaldehyde (Figure 1) and acetone (Figure 2) reactions, respectively.

Scheme 5. A reaction model of the acid-promoted aldol condensation.

larger electrophilic character of acetaldehyde than acetone. The large endergonic character for the formation of the enolate of acetone than that of acetaldehyde plays a similar role to the electrophilicity in the energy difference between TS2(at) and TS2(al). An interesting analysis can be also redrawn for the enolization step for the two carbonyl compounds. After TSs there is an energy crossing to enolates. Int1(al) is located below Int1(at), whereas TS1(at) is located below TS1(al). The presence of the electron-releasing methyl group on the enolate structure thermodynamically destabilizes the anionic structure. The aldehydes are more acidic than ketones. However, along the reaction path, this

methyl group has a different role to stabilize the TS associated to the C=C bond formation at the enolate by a hyperconjugative effect.^[13]

The OH⁻-promoted aldol reaction is reviewed. There are three elementary processes, C–H scission, C–C formation, and O–H formation. Cleavage or formation of each covalent bond takes place in each step.

The Acid-Promoted Reaction

Scheme 5 illustrates the model where inclusion of (H₂O)₈ is the same as in Scheme 4. The MeCHO molecule in the lower side is ready to be transformed into vinyl

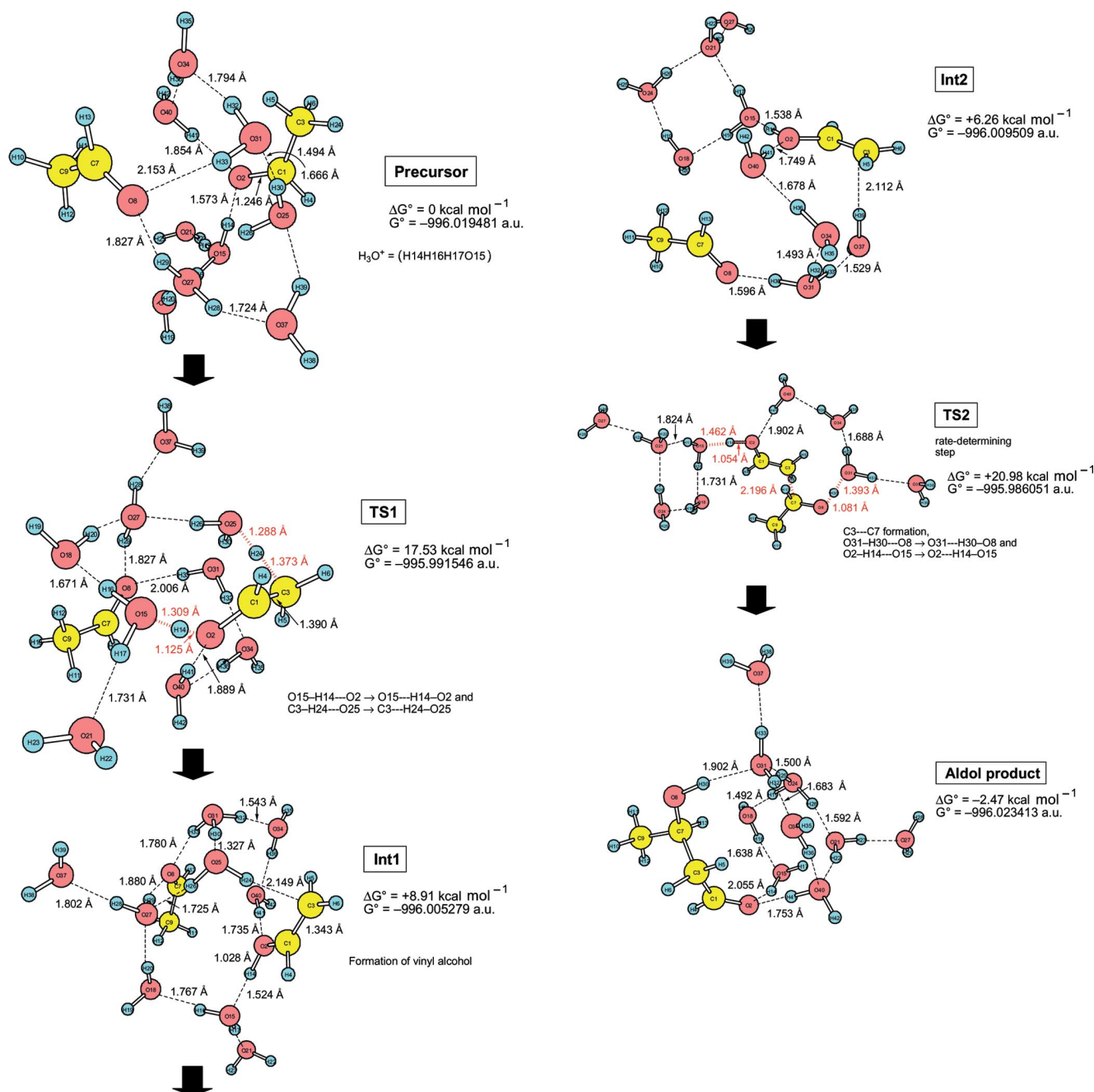


Figure 4. Geometric changes of the acid-catalyzed aldol reaction of (MeCHO)₂ + H₃O⁺ + (H₂O)₈ in Scheme 5.

alcohol. Figure 4 shows geometric changes. In the precursor, the hydronium ion H_3O^+ , ($\text{O}15\ \text{H}14\ \text{H}16\ \text{H}17$)⁺, is linked with the carbonyl oxygen atom O2. From the precursor, TS1 was obtained. At TS1, bond interchanges of $\text{O}15\cdots\text{H}14\cdots\text{O}2 \rightarrow \text{O}15\cdots\text{H}14\text{--O}2$ and $\text{C}3\cdots\text{H}24\cdots\text{O}25 \rightarrow \text{C}3\cdots\text{H}24\text{--O}25$ occur synchronously. The simultaneous bond interchanges have not been involved in the OH^- -promoted reaction. After TS1, the first intermediate (Int1) composed of acetaldehyde, vinyl alcohol, and $\text{H}_3\text{O}^+(\text{H}_2\text{O})_8$ is reached. The geometry of Int1 is rearranged to that of Int2 so that the subsequent C–C bond formation is ready. After Int2, the second TS (TS2) is brought about. Surprisingly, TS2 involves two bond interchanges, $\text{O}31\cdots\text{H}30\cdots\text{O}8 \rightarrow \text{O}31\cdots\text{H}30\text{--O}8$ and $\text{O}2\cdots\text{H}14\cdots\text{O}15 \rightarrow \text{O}2\cdots\text{H}14\text{--O}15$, as

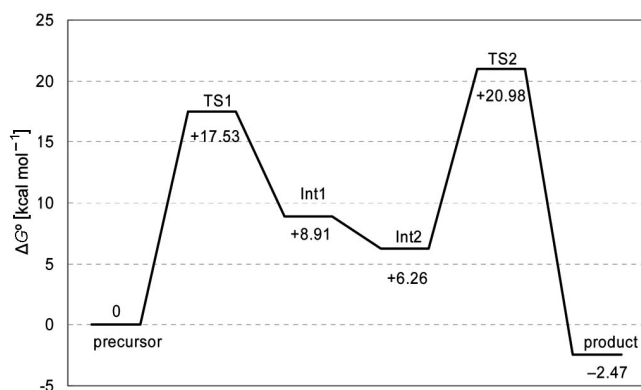
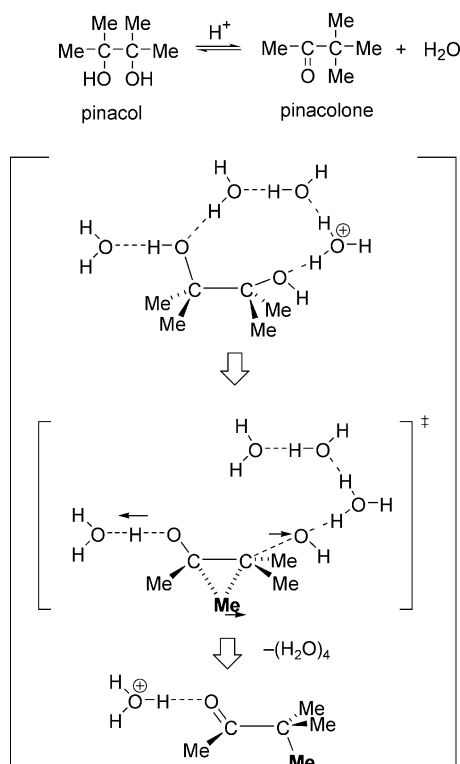


Figure 5. Energy diagram of Gibbs free energies ($T = 298.15\ \text{K}$ and $P = 1\ \text{atm}$) along the H_3O^+ promoted reaction of Figure 4.



Scheme 6. The concerted process of the pinacol rearrangement promoted by a hydrogen-bond circuit.

well as the $\text{C}3\cdots\text{C}7$ formation. After TS2, the aldol product is afforded. The H_3O^+ -promoted aldol reaction consists of two elementary processes.

Figure 5 exhibits the energy change of the H_3O^+ -promoted reaction. The rate-determining step is TS2, of which the energy ($+20.98\ \text{kcal mol}^{-1}$) is much larger than that of TS1 ($+12.22\ \text{kcal mol}^{-1}$) of the OH^- -promoted reaction (Figure 3). This result demonstrates that the acid-promoted aldol reaction is not so efficient as the base-promoted one.

The result of the two elementary processes found in the present calculation is inconsistent with the general idea of the three elementary processes depicted in Scheme 2. However, the former is consistent with our recent result for the acid-promoted pinacol rearrangement (Scheme 6).^[14] Proton relays through acid-containing hydrogen bonds are ready enough to make various bond interchanges synchronous.

Conclusion

In this work, OH^- - and H_3O^+ -promoted aldol reactions of acetaldehyde (and acetone with OH^-) were examined computationally. Eight water molecules were included to assure proton migrations through hydrogen bonds. Those were found to cover the charged reaction center and seem to be sufficient to describe bond interchanges reasonably. Further addition of water molecules to the outer region is expected to hardly alter the obtained results as judged from our previous work on ester hydrolysis.^[15] The OH^- -containing reaction was confirmed to consist of three elementary processes, (i), (ii), and (iii), as shown in Scheme 1. The rate-determining step in the reaction of acetaldehyde is C–H bond scission (TS1), whereas that of acetone is C–C bond formation (TS2). The H_3O^+ -containing reaction was found to have two elementary processes, which is different from the processes depicted in Scheme 2. The rate-determining step is C–C bond formation (TS2). The difference in the number of elementary processes between OH^- - and H_3O^+ -promoted reactions and the poor reactivity of the H_3O^+ reaction are considered in terms of u_+ , u_- (Table 1), and binding energies raised in the Introduction. The water association strength of OH^- is lower than that of H_3O^+ . The anion center may be transmitted to the substrate, which leads to the formation of the enolate. This anion may be a good nucleophile to make a C–C bond. On the contrary, the cation center is retained in H_3O^+ , and the protonated substrate cannot intervene throughout the reaction. Thus, the acid-catalyzed reaction cannot provide a good electrophile, which leads to poor reactivity. Resistance to the formation of the protonated substrate makes steps (ii) and (iii) synchronous in Scheme 2. The OH^- -promoted reaction of the aldehyde has the highest reactivity among the three.

Supporting Information (see footnote on the first page of this article): Cartesian coordinates of the structures in Figures 1, 2, and 4.

- [1] C. A. Wurtz, *Bull. Soc. Chim. Fr.* **1872**, 17, 436.
- [2] A. T. Nielsen, W. J. Houlihan, *Org. React.* **1968**, 16, 1.
- [3] P. Sykes, *A Guidebook to Mechanism in Organic Chemistry*, 5th ed., Longman, London, **1981**, ch. 8.4.4.
- [4] E. L. Coitiño, J. Tomasi, O. N. Ventura, *J. Chem. Soc. Faraday Trans.* **1994**, 90, 1745.
- [5] S. Kawaguchi, K. Nishimoto, *Introductory Physical Chemistry*, Kagaku Dojin, Japan, **1985**, ch. 8, p. 128.
- [6] P. Kebarle, S. K. Searles, A. Zolla, J. Scarborough, M. Arshadi, *J. Am. Chem. Soc.* **1967**, 89, 6393.
- [7] S. Yamabe, T. Minato, K. Hirao, *J. Chem. Phys.* **1984**, 80, 1576.
- [8] a) A. D. Becke, *J. Chem. Phys.* **1993**, 98, 5648; b) C. Lee, W. Yang, R. G. Parr, *Phys. Rev. B* **1998**, 37, 785.
- [9] a) K. Fukui, *J. Phys. Chem.* **1970**, 74, 4161; b) C. Gonzalez, H. B. Schlegel, *J. Phys. Chem.* **1989**, 90, 2154.
- [10] L. Onsager, *J. Am. Chem. Soc.* **1936**, 58, 1486.
- [11] M. J. Frisch, G. W. Trucks, H. B. Schlegel, G. E. Scuseria, M. A. Robb, J. R. Cheeseman, J. A. Montgomery Jr, T. Vreven, K. N. Kudin, J. C. Burant, J. M. Millam, S. S. Iyengar, J. Tomasi, V. Barone, B. Mennucci, M. Cossi, G. Scalmani, N. Rega, G. A. Petersson, H. Nakatsuji, M. Hada, M. Ehara, K. Toyota, R. Fukuda, J. Hasegawa, M. Ishida, T. Nakajima, Y. Honda, O. Kitao, H. Nakai, M. Klene, X. Li, J. E. Knox, H. P. Hratchian, J. B. Cross, V. Bakken, C. Adamo, J. Jaramillo, R. Gomperts, R. E. Stratmann, O. Yazyev, A. J. Austin, R. Cammi, C. Pomelli, J. W. Ochterski, P. Y. Ayala, K. Morokuma, G. A. Voth, P. Salvador, J. J. Dannenberg, V. G. Zakrzewski, S. Dapprich, A. D. Daniels, M. C. Strain, O. Farkas, D. K. Malick, A. D. Rabuck, K. Raghavachari, J. B. Foresman, J. V. Ortiz, Q. Cui, A. G. Baboul, S. Clifford, J. Cioslowski, B. B. Stefanov, G. Liu, A. Liashenko, P. Piskorz, I. Komaromi, R. L. Martin, D. J. Fox, T. Keith, M. A. Al-Laham, C. Y. Peng, A. Nanayakkara, M. Challacombe, P. M. W. Gill, B. Johnson, W. Chen, M. W. Wong, C. Gonzalez, J. A. Pople, *Gaussian 03*, Revision C.02, Gaussian, Inc., Wallingford CT, **2004**.
- [12] For instance, the C...C distance is 2.273 Å in the ethylene-butadiene Diels–Alder reaction. E. Goldstein, B. Beno, K. N. Houk, *J. Am. Chem. Soc.* **1996**, 118, 6036.
- [13] We appreciate a reviewer on this discussion.
- [14] S. Yamabe, N. Tsuchida, S. Yamazaki, *J. Comput. Chem.* **2007**, 28, 1561.
- [15] S. Yamabe, N. Tsuchida, Y. Hayashida, *J. Phys. Chem. A* **2005**, 109, 7216.

Received: July 25, 2007

Published Online: November 2, 2007